

Measurement of the Polarized Structure Function $\sigma_{LT'}$ for $p(\vec{e}, e'p)\pi^0$ in the $\Delta(1232)$ Resonance Region

K. Joo,^{1,2,3} L.C. Smith,² V.D. Burkert,³ R. Minehart,² G. Adams,³¹ P. Ambrozewicz,¹² E. Anciant,⁵ M. Anghinolfi,¹⁷ B. Asavapibhop,²⁴ G. Audit,⁵ T. Auger,⁵ H. Avakian,³ H. Bagdasaryan,²⁸ J.P. Ball,⁴ S. Barrow,¹³ M. Battaglieri,¹⁷ K. Beard,²¹ M. Bektasoglu,²⁷ M. Bellis,³¹ N. Benmouna,¹⁴ N. Bianchi,¹⁶ A.S. Biselli,⁷ S. Boiarinov,²⁰ S. Bouchigny,¹⁸ R. Bradford,⁷ D. Branford,¹¹ W.J. Briscoe,¹⁴ W.K. Brooks,³ C. Butuceanu,³⁸ J.R. Calarco,²⁵ D.S. Carman,²⁷ B. Carnahan,⁸ C. Cetina,¹⁴ L. Ciciani,²⁸ P.L. Cole,³⁵ A. Coleman,³⁸ D. Cords,³ P. Corvisiero,¹⁷ D. Crabb,² H. Crannell,⁸ J.P. Cummings,³¹ E. DeSanctis,¹⁶ R. DeVita,¹⁷ P.V. Degtyarenko,³ H. Denizli,²⁹ L. Dennis,¹³ K.V. Dharmawardane,²⁸ K.S. Dhuga,¹⁴ C. Djalali,³⁴ G.E. Dodge,²⁸ D. Doughty,⁹ P. Dragovitsch,¹³ M. Dugger,⁴ S. Dytman,²⁹ O.P. Dzyubak,³⁴ M. Eckhause,³⁸ H. Egiyan,³ K.S. Egiyan,³⁹ L. Elouadrhiri,⁹ A. Empl,³¹ P. Eugenio,¹³ R. Fatemi,² R.J. Feuerbach,⁷ J. Ficenec,³⁷ T.A. Forest,²⁸ H. Funsten,³⁸ S.J. Gaff,¹⁰ M. Gai,¹ G. Gavalian,²⁵ S. Gilad,²³ G.P. Gilfoyle,³³ K.L. Giovanetti,²¹ P. Girard,³⁴ C.I.O. Gordon,¹⁵ K. Griffioen,³⁸ M. Guidal,¹⁸ M. Guillo,³⁴ L. Guo,³ V. Gyurjyan,³ C. Hadjidakis,¹⁸ R.S. Hakobyan,⁸ J. Hardie,⁹ D. Heddle,⁹ P. Heimberg,¹⁴ F.W. Hersman,²⁵ K. Hicks,²⁷ R.S. Hicks,²⁴ M. Holtrop,²⁵ J. Hu,³¹ C.E. Hyde-Wright,²⁸ Y. Ilieva,¹⁴ M.M. Ito,³ D. Jenkins,³⁷ J.H. Kelley,¹⁰ M. Khandaker,²⁶ K.Y. Kim,²⁹ K. Kim,²² W. Kim,²² A. Klein,²⁸ F.J. Klein,^{3,8} A.V. Klimenko,²⁸ M. Klusman,³¹ M. Kossov,²⁰ L.H. Kramer,¹² Y. Kuang,³⁸ S.E. Kuhn,²⁸ J. Kuhn,⁷ J. Lachniet,⁷ J.M. Laget,⁵ D. Lawrence,²⁴ Ji Li,³¹ A.C.S. Lima,¹⁴ K. Lukashin,^{37,8} J.J. Manak,³ C. Marchand,⁵ L.C. Maximon,¹⁴ S. McAleer,¹³ J.W.C. McNabb,⁷ B.A. Mecking,³ S. Mehrabyan,²⁹ J.J. Melone,¹⁵ M.D. Mestayer,³ C.A. Meyer,⁷ K. Mikhailov,²⁰ M. Mirazita,¹⁶ R. Miskimen,²⁴ L. Morand,⁵ S.A. Morrow,⁵ M.U. Mozer,²⁷ V. Muccifora,¹⁶ J. Mueller,²⁹ L.Y. Murphy,¹⁴ G.S. Mutchler,³² J. Napolitano,³¹ R. Nasseripour,¹² S.O. Nelson,¹⁰ S. Niccolai,¹⁴ G. Niculescu,²⁷ I. Niculescu,²¹ B.B. Niczyporuk,³ R.A. Niyazov,²⁸ M. Nozar,³ G.V. O'Rielly,¹⁴ A.K. Opper,²⁷ M. Osipenko,¹⁷ K. Park,²² E. Pasyuk,⁴ G. Peterson,²⁴ S.A. Philips,¹⁴ N. Pivnyuk,²⁰ D. Pocanic,² O. Pogorelko,²⁰ E. Polli,¹⁶ S. Pozdniakov,²⁰ B.M. Preedom,³⁴ J.W. Price,⁶ Y. Prok,² D. Protopopescu,¹⁵ L.M. Qin,²⁸ B.A. Raue,¹² G. Riccardi,¹³ G. Ricco,¹⁷ M. Ripani,¹⁷ B.G. Ritchie,⁴ F. Ronchetti,¹⁶ P. Rossi,¹⁶ D. Rowntree,²³ P.D. Rubin,³³ F. Sabatié,⁵ K. Sabourov,¹⁰ C. Salgado,²⁶ J.P. Santoro,³⁷ V. Sapunenko,¹⁷ M. Sargsyan,¹² R.A. Schumacher,⁷ V.S. Serov,²⁰ Y.G. Sharabian,³⁹ J. Shaw,²⁴ S. Simionatto,¹⁴ A.V. Skabelin,²³ E.S. Smith,³ D.I. Sober,⁸ M. Spraker,¹⁰ A. Stavinsky,²⁰ S. Stepanyan,³⁹ P. Stoler,³¹ I.I. Strakovsky,¹⁴ S. Strauch,¹⁴ M. Taiuti,¹⁷ S. Taylor,³² D.J. Tedeschi,³⁴ U. Thoma,³ R. Thompson,²⁹ L. Todor,⁷ C. Tur,³⁴ M. Ungaro,³¹ M.F. Vineyard,³⁶ A.V. Vlassov,²⁰ K. Wang,² L.B. Weinstein,²⁸ H. Weller,¹⁰ D.P. Weygand,³ C.S. Whisnant,³⁴ E. Wolin,³ M.H. Wood,³⁴ A. Yegneswaran,³ J. Yun,²⁸ J. Zhao,²³ and Z. Zhou²³

(The CLAS Collaboration)

¹ University of Connecticut, Storrs, Connecticut 06269

² University of Virginia, Charlottesville, Virginia 22901

³ Thomas Jefferson National Accelerator Facility, Newport News, Virginia 23606

⁴ Arizona State University, Tempe, Arizona 85287-1504

⁵ CEA-Saclay, Service de Physique Nucléaire, F91191 Gif-sur-Yvette, Cedex, France

⁶ University of California at Los Angeles, Los Angeles, California 90095-1547

⁷ Carnegie Mellon University, Pittsburgh, Pennsylvania 15213

⁸ Catholic University of America, Washington, D.C. 20064

⁹ Christopher Newport University, Newport News, Virginia 23606

¹⁰ Duke University, Durham, North Carolina 27708-0305

¹¹ Edinburgh University, Edinburgh EH9 3JZ, United Kingdom

¹² Florida International University, Miami, Florida 33199

¹³ Florida State University, Tallahassee, Florida 32306

¹⁴ The George Washington University, Washington, DC 20052

¹⁵ University of Glasgow, Glasgow G12 8QQ, United Kingdom

¹⁶ INFN, Laboratori Nazionali di Frascati, Frascati, Italy

¹⁷ INFN, Sezione di Genova, 16146 Genova, Italy

¹⁸ Institut de Physique Nucleaire ORSAY, Orsay, France

¹⁹ Institute für Strahlen und Kernphysik, Universität Bonn, Germany

²⁰ Institute of Theoretical and Experimental Physics, Moscow, 117259, Russia

²¹ James Madison University, Harrisonburg, Virginia 22807

²² Kungpook National University, Taegu 702-701, South Korea

²³ Massachusetts Institute of Technology, Cambridge, Massachusetts 02139-4307

²⁴ University of Massachusetts, Amherst, Massachusetts 01003

²⁵ University of New Hampshire, Durham, New Hampshire 03824-3568

²⁶ Norfolk State University, Norfolk, Virginia 23504

²⁷ Ohio University, Athens, Ohio 45701

²⁸ Old Dominion University, Norfolk, Virginia 23529

²⁹ University of Pittsburgh, Pittsburgh, Pennsylvania 15260

³⁰ Università di ROMA III, 00146 Roma, Italy

³¹ Rensselaer Polytechnic Institute, Troy, New York 12180-3590

³² Rice University, Houston, Texas 77005-1892

³³ University of Richmond, Richmond, Virginia 23173

³⁴ University of South Carolina, Columbia, South Carolina 29208

³⁵ University of Texas at El Paso, El Paso, Texas 79968

³⁶ Union College, Schenectady, NY 12308

³⁷ Virginia Polytechnic Institute and State University, Blacksburg, Virginia 24061-0435

³⁸ College of William and Mary, Williamsburg, Virginia 23187-8795

³⁹ Yerevan Physics Institute, 375036 Yerevan, Armenia

The polarized longitudinal-transverse structure function $\sigma_{LT'}$ has been measured in the $\Delta(1232)$ resonance region at $Q^2 = 0.40$ and 0.65 GeV². Data for the $p(\vec{e}, e'p)\pi^0$ reaction were taken at Jefferson Lab with the CEBAF Large Acceptance Spectrometer (CLAS) using longitudinally polarized electrons at an energy of 1.515 GeV. For the first time a complete angular distribution was measured, permitting the separation of different non-resonant amplitudes using a partial wave analysis. Comparison with previous beam asymmetry measurements at MAMI indicate a deviation from the predicted Q^2 dependence of $\sigma_{LT'}$ using recent phenomenological models.

PACS numbers: PACS : 13.60.Le, 12.40.Nn, 13.40.Gp

The $\gamma^*p \rightarrow \Delta^+(1232)$ transition has long served as a benchmark for testing nucleon models. In the $SU(6)$ symmetric quark model, this strong magnetic dipole excitation is described as originating from a single quark spin flip. Residual spin-dependent and tensor-type interactions between the quarks are needed to explain the $N - \Delta$ mass difference and the small quadrupole transition strength observed in partial wave analyses of experimental pion electroproduction data [1, 2, 3]. Understanding the origin of these residual interactions and their role in resonance formation and decay is a fundamental challenge for modern QCD-inspired hadronic models.

In particular, the dynamical effects of the pion cloud are predicted to strongly modify the electromagnetic couplings at sufficiently low Q^2 . Chiral-quark and bag models that incorporate pion couplings [4, 5, 6, 7] generally describe the $\Delta(1232)$ photocoupling multipoles better than a purely quark/gluon framework [8, 9]. Recent dynamical models derived from effective chiral Lagrangians explicitly treat pion multiple scattering [10, 11] and predict strong modifications to both resonant and non-resonant amplitudes. The important role of the pion cloud in electromagnetic interactions has been emphasized recently in heavy baryon chiral perturbation theory [12] and unquenched lattice QCD [13].

Unfortunately, cross section measurements alone do not provide sufficient information to separate the $\Delta(1232)$ excitation reaction mechanisms from non-resonant backgrounds and the tails of higher-mass resonances. Single spin polarization observables, on the other hand, are directly sensitive to the interference between resonant and non-resonant processes and together with precise cross sections can provide powerful constraints to models.

In this Rapid Communication we report new measure-

ments of the longitudinal-transverse polarized structure function $\sigma_{LT'}$ obtained in the $\Delta(1232)$ resonance region using the $p(\vec{e}, e'p)\pi^0$ reaction. Recent measurements of polarization observables [14, 15, 16, 17] and unpolarized cross sections [2, 18] for $Q^2 < 0.2$ GeV² show disagreement with some dynamical models near the $\Delta(1232)$ peak. However, so far only narrow angular and kinematic ranges have been studied, yielding few clues as to the origin of the discrepancy. The present experiment was performed at four-momentum transfers $Q^2 = 0.40$ and 0.65 GeV² and covers a range of invariant mass $W = 1.1 - 1.3$ GeV with full angular coverage in $\cos \theta_\pi^*$ and ϕ_π^* in the $p\pi^0$ center-of-mass (c.m.).

The data were taken at the Thomas Jefferson National Accelerator Facility (Jefferson Lab) using a 1.515 GeV, 100% duty-cycle beam of longitudinally polarized electrons incident on liquid hydrogen target. The electron polarization was determined by frequent Møller polarimeter measurements to be $0.69 \pm 0.009(\text{stat.}) \pm 0.013(\text{syst.})$. Scattered electrons and protons were detected in the CLAS spectrometer [19]. Electron triggers were enabled through a hardware coincidence of the gas Cerenkov counters and the lead-scintillator electromagnetic calorimeters. Protons were identified using momentum reconstruction in the tracking system and time of flight from the target to the scintillators. Software fiducial cuts were used to exclude regions of non-uniform detector response. Kinematic corrections were applied to compensate for drift chamber misalignments. The $p\pi^0$ final state was identified by requiring the missing neutral to have a mass squared between -0.01 and 0.05 GeV². Background from elastic Bethe-Heitler radiation was suppressed to below 1% using a combination of cuts on missing mass and ϕ_π^* near $\phi_\pi^* = 0^\circ$. Target window backgrounds were suppressed with cuts

on the reconstructed $e'p$ target vertex.

In the one-photon-exchange approximation, the electroproduction cross section factorizes as follows:

$$\frac{d^5\sigma}{dE_{e'}d\Omega_{e'}d\Omega_{\pi}^*} = \Gamma_v \frac{d^2\sigma^h}{d\Omega_{\pi}^*}, \quad (1)$$

where Γ_v is the virtual photon flux and $d^2\sigma^h$ is the differential cross section for $\gamma^*p \rightarrow p\pi^0$ with electron beam helicity ($h = \pm 1$). For an unpolarized target, $d^2\sigma^h$ depends on the transverse (ϵ) and longitudinal (ϵ_L) polarization of the virtual photon through five structure functions: σ_T, σ_L and their interference terms σ_{TT}, σ_{LT} and $\sigma_{LT'}$:

$$\begin{aligned} \frac{d^2\sigma^h}{d\Omega_{\pi}^*} &= \frac{p_{\pi}^*}{k_{\gamma}^*} (\sigma_0 + h\sqrt{2\epsilon_L(1-\epsilon)}\sigma_{LT'} \sin\theta_{\pi}^* \sin\phi_{\pi}^*), \\ \sigma_0 &= \sigma_T + \epsilon_L\sigma_L + \epsilon\sigma_{TT} \sin^2\theta_{\pi}^* \cos 2\phi_{\pi}^* \\ &\quad + \sqrt{2\epsilon_L(1+\epsilon)}\sigma_{LT} \sin\theta_{\pi}^* \cos\phi_{\pi}^*, \end{aligned} \quad (2)$$

where $(p_{\pi}^*, \theta_{\pi}^*, \phi_{\pi}^*)$ are the π^0 c.m. momentum, polar and azimuthal angles, $\epsilon = (1 + 2|\vec{q}'|^2 \tan^2(\theta_e/2)/Q^2)^{-1}$, $\epsilon_L = (Q^2/|k^*|^2)\epsilon$, and k_{γ}^* and $|k^*|$ are the virtual photon c.m. momentum and equivalent energy.

The structure functions σ_{LT} and $\sigma_{LT'}$ determine the real and imaginary parts of bilinear products between longitudinal and transverse amplitudes:

$$\sigma_{LT} : \text{Re}(L^*T) = \text{Re}(L)\text{Re}(T) + \text{Im}(L)\text{Im}(T) \quad (3)$$

$$\sigma_{LT'} : \text{Im}(L^*T) = \text{Re}(L)\text{Im}(T) - \text{Im}(L)\text{Re}(T). \quad (4)$$

Detection of a weak non-resonant background underlying the peak of the $\Delta(1232)$ can be enhanced through its interference in $\sigma_{LT'}$ with the strong transverse magnetic multipole $\text{Im}(M_{1+})$. Sensitivity to real backgrounds is suppressed in σ_{LT} due to the vanishing of $\text{Re}(M_{1+})$ at the resonance pole.

Extraction of $\sigma_{LT'}$ was made through a measurement of the electron beam asymmetry $A_{LT'}$:

$$A_{LT'} = \frac{d^2\sigma^+ - d^2\sigma^-}{d^2\sigma^+ + d^2\sigma^-} \quad (5)$$

$$= \frac{\sqrt{2\epsilon_L(1-\epsilon)}\sigma_{LT'} \sin\theta_{\pi}^* \sin\phi_{\pi}^*}{\sigma_0}. \quad (6)$$

$A_{LT'}$ was obtained by dividing the measured asymmetry A_m by the magnitude of the electron beam polarization P_e :

$$A_{LT'} = \frac{A_m}{P_e} \quad (7)$$

$$A_m = \frac{N_{\pi^+} - N_{\pi^-}}{N_{\pi^+} + N_{\pi^-}}, \quad (8)$$

where N_{π}^{\pm} is the number of π^0 events per incident electron for each electron beam helicity state. $A_{LT'}$ was determined for individual bins of $(Q^2, W, \cos\theta_{\pi}^*, \phi_{\pi}^*)$. Normalization factors cancel in Eq. 6, and since acceptance studies showed no significant helicity or bin size dependence, acceptance factors canceled in A_m as well. This

leaves A_m largely free from systematic errors. Radiative corrections were applied for each bin using the program recently developed by A. Afanasev *et al.* for exclusive pion electro-production [20]. Corrections were also applied to compensate for cross section variations over the width of each bin. The corrected $A_{LT'}$ was multiplied by the unpolarized cross section σ_0 . A parameterization of σ_0 was used, which was obtained from the SAID PR01 solution [21] fitted to previously measured CLAS data and world data. The structure function $\sigma_{LT'}$ was then extracted using Eq. 6 by fitting the ϕ_{π}^* distributions. Systematic errors for $\sigma_{LT'}$ were dominated by uncertainties in determination of the electron beam polarization and the parameterized unpolarized cross section σ_0 . The systematic error for A_m is negligible in comparison. Quadratic addition of the individual contributions yields a total relative systematic error of $< 6\%$.

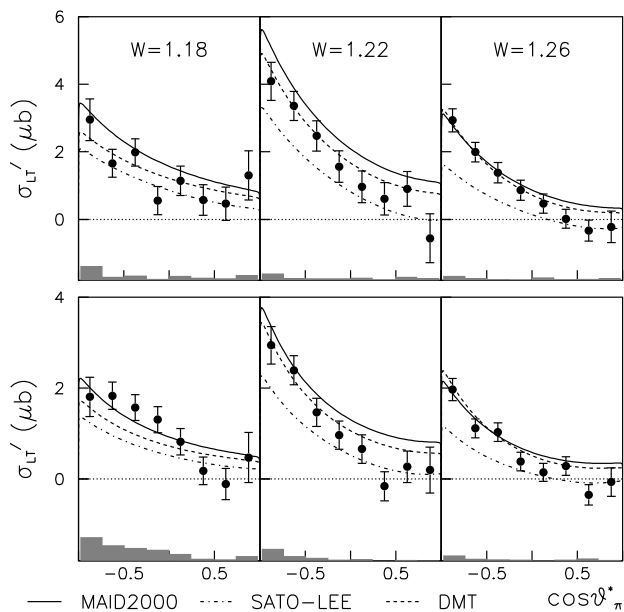


FIG. 1: CLAS measurement (\bullet) of $\sigma_{LT'}$ versus $\cos\theta_{\pi}^*$ extracted at $Q^2=0.40$ GeV 2 (top) and $Q^2=0.65$ GeV 2 (bottom). Curves show model predictions. Shaded bars show systematic errors.

Fig. 1 shows $\sigma_{LT'}$ extracted at $Q^2=0.40$ GeV 2 and $Q^2=0.65$ GeV 2 , where the $\cos\theta_{\pi}^*$ dependence is plotted for W bins of 1.18, 1.22, and 1.26 GeV. The measured angular distributions show a strong backward peaking for W bins around the $\Delta(1232)$ mass. The curves show predictions from recent models [10, 22, 23] which use different methods to satisfy unitarity in the π^0p final state. These models, which are fitted to previous photo- and unpolarized electro-production data, include backgrounds arising from Born diagrams and t -channel vector meson exchange. The Sato-Lee [10] and Dubna-Mainz-Taipei [22] (DMT) models use an off-shell πN re-

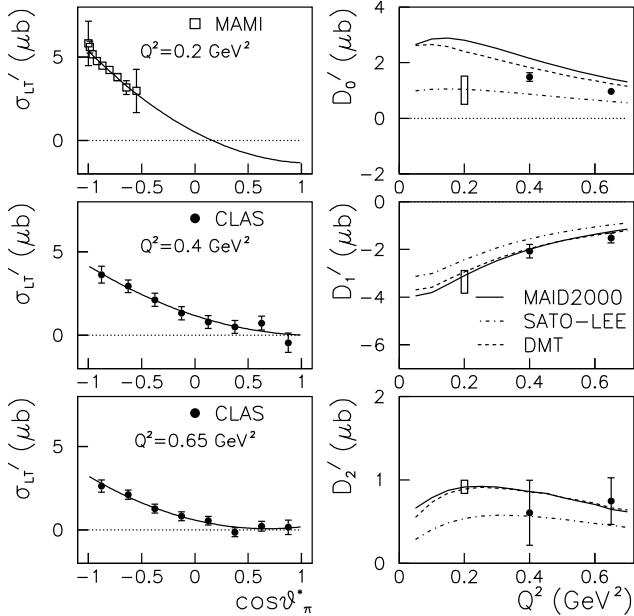


FIG. 2: LEFT: Fits to $\sigma_{LT'}$ angular distributions measured by CLAS (middle, bottom) and MAMI (top) at $W = 1232 \text{ GeV}$ using Eq.(9). See text for details. RIGHT: Q^2 dependence of Legendre moments of $\sigma_{LT'}$. Curves show model predictions. Data points are the present CLAS measurement. Vertical bars at $Q^2=0.2 \text{ GeV}^2$ show moments obtained from model constrained fits to MAMI data [16].

action theory to calculate unitarity corrections, while the more phenomenological MAID2000 model [23] incorporates πN phases directly into the background amplitudes. While the models describe the data qualitatively, none of the calculations is able to describe both the overall magnitude and the slope of the measured c.m. angular distributions consistently.

A more quantitative comparison was made through fitting the extracted $\sigma_{LT'}$ angular distributions using the Legendre expansion:

$$\sigma_{LT'} = D'_0 + D'_1 P_1(\cos\theta_\pi^*) + D'_2 P_2(\cos\theta_\pi^*), \quad (9)$$

where $P_l(\cos\theta_\pi^*)$ is the l^{th} -order Legendre polynomial and D'_l is the corresponding Legendre moment. Each moment can be decomposed into interference terms involving the leading-order magnetic ($M_{l\pi\pm}$), electric ($E_{l\pi\pm}$), and scalar ($S_{l\pi\pm}$) multipoles:

$$D'_0 = -\text{Im}((M_{1-} - M_{1+} + 3E_{1+})^* S_{0+} + E_{0+}^*(S_{1-} - 2S_{1+}) + \dots) \quad (10)$$

$$D'_1 = -6\text{Im}((M_{1-} - M_{1+} + E_{1+})^* S_{1+} + E_{1+}^* S_{1-} + \dots) \quad (11)$$

$$D'_2 = -12\text{Im}((M_{2-} - E_{2-})^* S_{1+} + 2E_{1+}^* S_{2-} + \dots), \quad (12)$$

where l_π is the $\pi^0 p$ angular momentum whose coupling with the nucleon spin is indicated by \pm .

Fig. 2 shows typical fits to $\sigma_{LT'}$ angular distributions near the peak of the $\Delta(1232)$ resonance (left), while the Q^2 dependence of the extracted Legendre moments is compared to model predictions (right). The largest disagreement with models clearly occurs for D'_0 , which is dominated by interference terms involving s -wave πN multipoles. The CLAS data also require $D'_2 \neq 0$. The fitted D'_2 strength has the same sign and overall magnitude as the model predictions, although we cannot differentiate between the models due to large statistical uncertainties. No evidence for d -waves was observed in our measurement of σ_{LT} [1].

We also compare our fit results with a recent MAMI measurement [16] of the beam asymmetry $A_{LT'}$ at $Q^2 = 0.2 \text{ GeV}^2$. The published MAMI angular distribution was converted to $\sigma_{LT'}$ using Eq. 6 and MAID2000 for the unpolarized cross section σ_0 . Since the MAMI data do not have sufficient angular coverage to determine D'_2 , the fit was performed by constraining D'_2 relative to D'_1 using MAID2000. With D'_2 fixed, the remaining Legendre moments estimated from the MAMI data can be compared to the Q^2 trend of the CLAS data (Fig. 2, right). Both data sets suggest an anomalous behavior for D'_0 with respect to the models. However, a recent BATES measurement [17] of $\sigma_{LT'}$ at $Q^2 = 0.127 \text{ GeV}^2$ and $\theta_\pi^* = 129^\circ$ found good agreement with MAID2000 and DMT, although no angular distributions were reported.

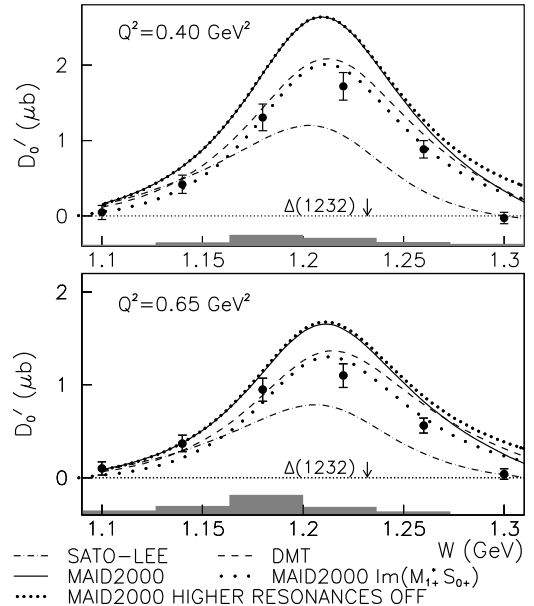


FIG. 3: CLAS measurement (\bullet) of Legendre moment D'_0 vs. W (GeV). Curves show recent model calculations that include contributions from multipoles up to angular momentum $l_\pi = 5$. Shaded bars show systematic errors.

Fig. 3 and Fig. 4 show the W dependence of the fitted Legendre moments, D'_0 and D'_1 , respectively. Both moments show strong resonant behavior, suggesting dom-

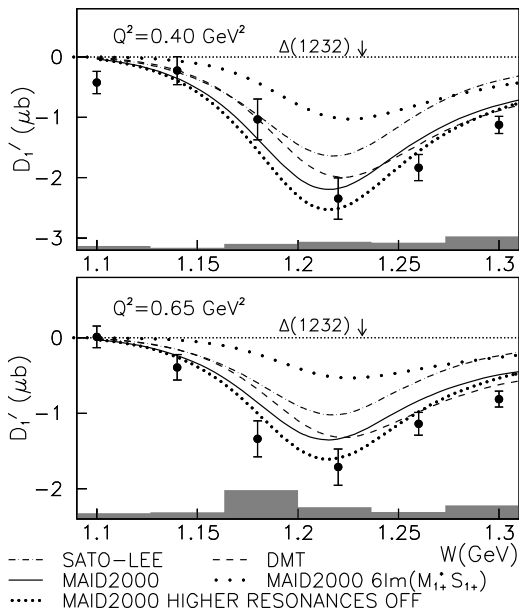


FIG. 4: CLAS measurement (\bullet) of Legendre moment D'_1 vs. W (GeV). See Fig. 3 for details.

inance of interference terms involving the multipoles of the $\Delta(1232)$. Our measurement of D'_0 is substantially below the predictions of MAID2000, and in closer agreement with the DMT dynamical model at $W = 1.18$ GeV, while the Sato-Lee prediction is smaller still. For increasing W , our data fall below the DMT curve, while none of the models describes the W dependence well. Note that contributions of higher resonances to D'_0 are negligible except near $W=1.30$ GeV. Figure 4 shows the fit results for D'_1 . Here our comparison with models shows some Q^2 dependence. Better agreement with the dynamical models occurs below the $\Delta(1232)$ at $Q^2 = 0.4$ GeV 2 , while at $Q^2 = 0.65$ GeV 2 all of the W points are systematically larger than the predictions.

The large differences between the model predictions

for D'_0 arise from the term $Im(M_{1+}^* S_{0+})$, which produces 70-75% of the total strength in MAID2000. In contrast, D'_1 is more sensitive to higher resonances, which contribute 15-20% in MAID2000 (coming mainly from $Im(M_{1-}^* S_{1+})$), while $Im(M_{1+}^* S_{1+})$ accounts for $\approx 40\%$ of the total strength. The S_{0+} multipole is an important background affecting the extraction of the $\gamma^* p \rightarrow \Delta(1232)$ $C2$ Coulomb quadrupole transition, and is sensitive to choices of πNN coupling and contributions from final state πN rescattering [23]. Unfortunately, a simple rescaling of the S_{0+} strength, as suggested in Ref. [16], is not sufficient to account for the inferred Q^2 dependence of D'_0 .

In summary, complete angular distributions for the polarized structure function $\sigma_{LT'}$ were measured for the first time, using the $p(\bar{e}, e'p)\pi^0$ reaction. In accordance with measurements at lower Q^2 [14, 15, 16, 17], evidence for significant non-resonant background in the $\Delta(1232)$ region is seen. A departure from the predicted Q^2 dependence of various effective Lagrangian based models is seen at the $\Delta(1232)$ peak when the CLAS data are compared to the MAMI data at $Q^2 = 0.2$ GeV 2 . Examination of the Legendre moments D'_0 and D'_1 shows the discrepancies are largest for D'_0 . CLAS measurements in the Q^2 range of 0.1-0.4 GeV 2 and also for $W > 1.3$ GeV are currently being analyzed to provide more information on the form factors of the underlying multipoles.

We acknowledge the efforts of the staff of the Accelerator and Physics Divisions at Jefferson Lab in their support of this experiment. This work was supported in part by the U.S. Department of Energy and National Science Foundation, the Emmy Noether Grant from the Deutsche Forschungsgemeinschaft, the French Commissariat a l'Energie Atomique, the Italian Istituto Nazionale di Fisica Nucleare, and the Korea Research Foundation. The Southeastern Universities Research Association (SURA) operates the Thomas Jefferson Accelerator Facility for the United States Department of Energy under contract DE-AC05-84ER40150.

-
- [1] K. Joo et al., Phys. Rev. Lett. **88**, 122001 (2002).
 - [2] C. Mertz et al., Phys. Rev. Lett. **86**, 2963 (2001).
 - [3] V. V. Frolov et al., Phys. Rev. Lett. **82**, 45 (1999).
 - [4] K. Bermuth et al., Phys. Rev. D **37**, 89 (1988).
 - [5] H. Walliser and G. Holzwarth, Z. Phys. **A357**, 317 (1997).
 - [6] A. Silva et al., Nucl. Phys. **A675**, 637 (2000).
 - [7] L. Amoreira, P. Alberto, and M. Fiolhais, Phys. Rev. C **62**, 045202 (2000).
 - [8] S. Capstick and G. Karl, Phys. Rev. D **41**, 2767 (1990).
 - [9] N. Isgur, G. Karl, and R. Koniuk, Phys. Rev. D **25**, 2394 (1982).
 - [10] T. Sato and T.-S.H. Lee, Phys. Rev. C **63**, 055201 (2001).
 - [11] S. S. Kamalov et al., Phys. Rev. C **64**, 032201(R) (2001).
 - [12] G. Gellas et al., Phys. Rev. D **60**, 054022 (1999).
 - [13] C. Alexandrou et al., hep-lat/0209074.
 - [14] T. Pospischil et al., Phys. Rev. Lett. **86**, 2959 (2001).
 - [15] G. Warren et al., Phys. Rev. C **58**, 3722 (1998).
 - [16] P. Bartsch et al., Phys. Rev. Lett. **88**, 142001 (2002).
 - [17] C. Kunz et al., Phys. Lett. **B564**, 21 (2003).
 - [18] N.F. Sparveris et al., Phys. Rev. C **67**, 058201 (2003).
 - [19] B. Mecking et al., Nucl. Inst. Meth. **503**, 513 (2003).
 - [20] A. Afanasev, I. Akushevich, V. Burkert, and K. Joo, Phys. Rev. D **66**, 074004 (2002).
 - [21] R. Arndt, I. Strakovsky, and R. Workman, nucl-th/0110001.
 - [22] S. S. Kamalov and S. N. Yang, Phys. Rev. Lett. **83**, 4494 (1999).
 - [23] D. Drechsel et al., Nucl. Phys. **A645**, 145 (1999), URL www.kph.uni-mainz.de/MAID/.